A Novel Threshold Calibration Methodology for Quanta Image Sensors (QIS)

Dakota A. Starkey[1], Jiaju Ma[2], Saleh Masoodian[2] and Eric R. Fossum[1]

[1]Thayer School of Engineering, Dartmouth College, Hanover, NH, USA, [2]Gigajot Technology Inc., Pasadena, CA, USA
Contact: Dakota.A.Starkey@dartmouth.edu

Abstract—**A new characterization methodology for characterizing conversion gain and read noise in deep sub-electron read noise pixels using only a binary output data stream is proposed. This technique seeks to address the unique issue of calibrating the thresholding circuit in a single bit Quanta Image Sensor device without the need for a calibrated light source.**

I. INTRODUCTION

THE Quanta Image Sensor (QIS) was proposed in 2005 as a new paradigm in solid-state image sensing to maintain high dynamic range and SNR while pixel pitches and full well capacity continues to shrink [1]. In the envisioned concept, a large array of very small sub-diffraction limit pixels, called jots, is used to spatially oversample the incident photons of light [2]. In addition to their small size, these jots would also be sensitive enough to detect the absorption of a single photon. In each frame the output voltage from each jot is digitized into a '1' or '0' depending on whether or not 1 or more photons was collected in that frame. To reconstruct the data into an image, many binary frames can be captured in quick succession and be digitally recombined in post processed [3] [4].

The single bit QIS concept relies on single-photon sensitivity. That is to say that the voltage signal generated per collected photoelectron needs to be large enough to reliably overcome the inherent background noise in the readout electronics. Single photon avalanche diodes (SPAD) achieve single-photon sensitivity by leveraging electron avalanche multiplication [5]. This drastically increases the voltage signal generated per photon and gives SPADs an very fast response time on the order of 10s-100s of picoseconds [6]. However, this architecture incurs several drawbacks in terms of a lack of CMOS compatibility due to high voltages and large pitch size. In 2015 a CMOS-compatible pump-gate (PG) jot and tapered reset gate (TPG) jot were reported demonstrating photon-counting sensitivity without avalanche gain using a 1.4μm pixel pitch [7] with further improvements and a 1.1μm pitch design reported in 2017 [8]. Based on these promising results, the jot devices are the leading candidate for use in a QIS device.

In addition to the photon-counting sensitivity provided by the TPG jots, a QIS device also requires a comparator to condition the jot output to a '1' or a '0' [9]. The threshold level for these circuits needs to be accurately set to the voltage corresponding to 0.5e-. For SPADs, the percent variation in CG is low enough such that a single threshold voltage can be used for the entire array. However, for the TPG jot device, this variation in CG can be large enough that a global threshold for the entire array would give inaccurate results [10].

In this work, we present a new methodology for calibrating a jot-based QIS device. Unlike conventional CMOS image sensor circuit calibration techniques [11] this new technique incorporates both the pixel and the comparator for more accurate results. Using this new technique, the CG of each pixel can be used for comparator calibration, without the need for any additional readout circuitry.

II. PHOTON COUNTING STATISTICS

The statistical characteristics of photon-counting sensors both without [12] and with [13] Gaussian read noise have revealed unique characteristics about these types of sensors. For sensors with input-referred read noise below 0.45e- rms, distinct peaks and valleys can be seen in the output analog distribution under a stable illumination as shown in Figure 1. The overlapping fit is given by the analytic equation:

$$P[U] = \sum_{k=0}^{\infty} \frac{1}{u_n\sqrt{2\pi}} exp\left(\frac{-(U-k)^2}{2u_n^2}\right) \frac{e^{-H}H^k}{k!}$$

Also called the photon-counting histogram, this distribution can be used to extract key pixel information such as CG and read noise based on the peak-to-peak separation and the valley-to-peak ratio. As the read noise decreases, the width of the Gaussian at each peak will also decrease, leading to less overlap and a smaller valley. Because of this, the photon-counting error rate is

closely tied to the read noise of the jot.

From this, a threshold voltage corresponding to 0.5e- should give data with the minimum photon-counting error rate. The Gaussian spreading at each peak will result in false positive counts or false negative counts if the threshold voltage is set too low or too high, respectively. Figure 2 shows the effects of threshold level on the bit error rate. From this plot we can see that any deviation from a threshold of 0.5e- will increase the BER, particularly at lower read noise levels.

Usually the least significant bit (LSB) of readout ADCs used in CMOS image sensors can be calibrated by injecting an off-chip signal, as this value is typically not closely related to the CG of the pixel. However, we cannot know what each pixel's CG will be after fabrication. A separate analog readout chain could be included on-chip at the cost of chip area and additional design time and complexity. Instead, a method that uses light as the "injected signal" and looks at the change in the output binary values could provide the necessary information without requiring additional components.

Depending on the CG, the comparator threshold and the incident light intensity, the resulting output bit density, or the percentage of '1's that appear in a given number of samples will change. From a mathematical standpoint, the comparator will act on the probability density shown in Figure 1 by integrating this function for all voltages greater than the threshold voltage. If the detector is left under a stable illumination and the threshold voltage is swept, one would be able to recover the cumulative density function corresponding to the probability density function like the one in Figure 1.

The underlying probability density function can then be recovered using numerical differentiation and characterized by the PCH methodology as outlined in [13]. When performing this sweep, care must be taken in selecting the appropriate sweep resolution, as this will directly impact the accuracy of the recovered probability density function. To test the limits of this methodology, cumulative density functions were constructed from analytic PCH data and numerical differentiation with different step sizes was used to recover the probability density function. The PCH methodology was then used to characterize the data. Figure 3 and 4 shows the accuracy in the extracted CG and read noise as a function of the threshold sweep resolution using H=1 and CG=350µV/e-. We note that for threshold sweep resolutions higher than 175µV (or 0.5e-), the probability density function could not be recovered using numerical differentiation. From this, sweep resolutions of <0.4e- should be used for accurate characterization. These results were similar for CG=700µV/e- and CG=1000µV/e- with similar limitations. While the error

in the extracted read noise is fairly high, that parameter is less of a concern for calibration.

III. EXPERIMENTAL DATA

To validate this data processing methodology, a first generation QIS camera module made by Gigajot Technology Inc was used to collect photon-counting analog data. At the time, a photon-counting pixel paired with an adjustable threshold comparator was not available. Instead, the analog data from the sensor was quantized in data processing to simulate the data coming from a single bit ADC. Figure 5(a) shows the resulting cumulative density function for the full 1024x1024 pixel array using a global threshold voltage that reflects the average of the array. Figure 5(b) shows the extracted probability density function (green) and the analytic fit determined by the PCH methodology (purple). We can see from Figure 5(b) that there are some significant points of mismatch between the analytic curve and the experimental data.

To test the effect of the proposed calibration ideology, the analog data from each pixel was used to characterize its CG. For the proposed technique, the cumulative density function would be used to characterized the CG of each pixel. Using this data, the full array data was re-processed into binary data using a unique CG value for each pixel. The results of the extracted probability density (green) and the analytic fit (purple) is shown in Figure 6. The experimental data shows a better match to the theoretical expectation.

Further testing of this methodology was also done using test images. Figure 7 shows a set of calibrated (per pixel CG for quantization) and uncalibrated (global CG based on average) using the same camera. For these images, the QIS concept is further explored by demonstrating the effect of different jot cubicle sizes. These are noted in a X x Y x T format where X and Y refer to the number of jots that are summed in the vertical and horizontal direction while T refers to the number of frames in the sum. From these images, we see little difference in the overall quality in the two sets of images, likely due to the small conversion gain variation observed in these devices (~2.3%).

IV. CONCLUSION

In this paper, a novel characterization technique for characterizing binary data from photon-counting pixels without the need for any analog readout chain is reported. The theory behind this technique is explored and its limitations for implementation are determined through numerical simulations. Experimental analog photon-counting data is used to validate the improvements realized by this approach.

V. References

[1] E. R. Fossum, "What to do with sub-diffraction-limit (SDL) pixels?—A proposal for a gigapixel digital film sensor (DFS)," *IEEE Workshop on Charge-Coupled Devices and Advanced Image Sensors*, pp. 214-217, 2005.

[2] E. R. Fossum, J. Ma, S. Masoodian, l. Anzagira and R. Zizza, "The Quanta Image Sensor: Every Photon Counts," *Sensors*, vol. 16, no. 1260, pp. 1-25, 2016.

[3] S. H. Chan, O. A. Elgendy and X. Wang, "Images from bits: non-iterative image reconstruction for quanta image sensors," *Sensors*, vol. 16, no. 11, pp. 1961-1982, 2016.

[4] J. H. Choi, O. A. Elgendy and S. H. Chan, "Image Reconstruction for Quanta Image Sensors using Deep Neural Networks," in *IEEE International Conference on Acoustics, Speech & Signal Processing*, Calgary, Alberta, Canada, 2018.

[5] N. A. W. Dutton, I. Gyongy, L. Parmesan and R. K. Henderson, "Single Photon Counting Performance and Noise Analysis of CMOS SPAD-Based Image Sensors," *Sensors*, vol. 16, no. 1122, pp. 1-17, 2016.

[6] I. Gyongy, N. Calder, A. Davies, N. A. W. Dutton, R. R. Duncan, C. Rickman, P. Dalgarno and R. K. Henderson, "A 32x32-Pixel Array with In-Pixel Photon Counting and Arrival Time Measurement in the Analog Domain," *IEEE Transactions on Electron Device*, vol. 65, no. 2, pp. 547-554, 200.

[7] J. Ma, D. A. Starkey, A. Rao, K. Odame and E. R. Fossum, "Characterization of Quanta Image Sensor Pump-Gate Jots With Deep Sub-Electron Read Noise," *Journal of the Electron Device Society*, vol. 3, no. 6, pp. 472-480, 2015.

[8] J. Ma, S. Masoodian, D. A. Starkey and E. R. Fossum, "Photon-number-resolving megapixel image sensor at room temperature without avalanche gain," *Optica*, vol. 4, no. 12, pp. 1474-1481, 2017.

[9] S. Masoodian, A. Rao, J. Ma, K. Odame and E. R. Fossum, "A 2.5 pJ/b binary image sensor as a pathfinder for quanta image sensors," *IEEE Transactions on Electron Devices*, vol. 63, no. 1, pp. 100-105, 2016.

[10] E. R. Fossum, "Photon Counting Error Rates in Single-Bit and Multi-Bit Quanta Image Sensors," *IEEE Journal of Electron Devices*, vol. 4, no. 3, pp. 136-143, 2016.

[11] M. F. Snoeij, A. J. Theuwissen, K. A. Makinwa and J. H. Huijsing, "Multiple-ramp column-parallel ADC architectures for CMOS image sensors," *IEEE J. Solid-State Circuits (JSSC)*, vol. 42, no. 12, pp. 2968-2977, 2007.

[12] E. R. Fossum, "Application of Photon Statistics to the Quanta Image Sensor," in *2013 International Image Sensor Workshop*, Snowbird, Utah, 2013.

[13] D. A. Starkey and E. R. Fossum, "Determining conversion gain and read noise using a photon-counting histogram method for deep sub-electron read noise image sensors," *IEEE Journal of Electron Devices*, vol. 4, no. 3, pp. 129-135, 2016.
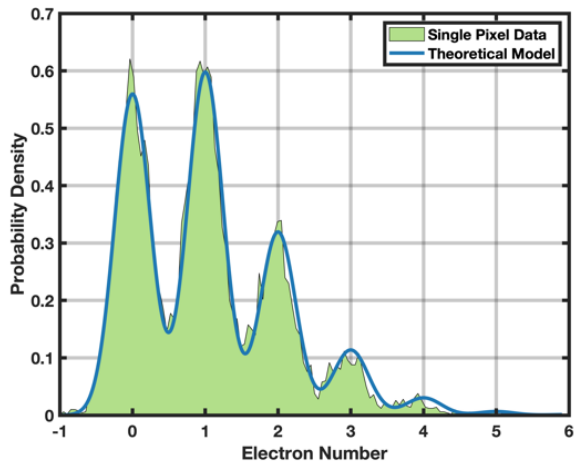
Figure 1: Experimental probability density function of single pixel readout 10,000 times with 0.245e- rms read noise.
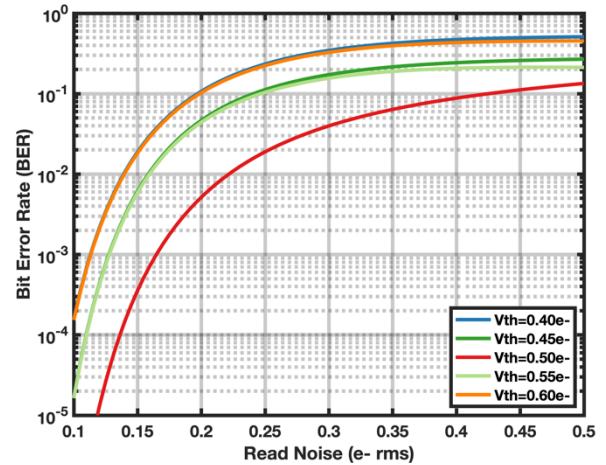

Figure 2: Simulated effects of threshold mismatch on the bit-error rate as a function of read noise.
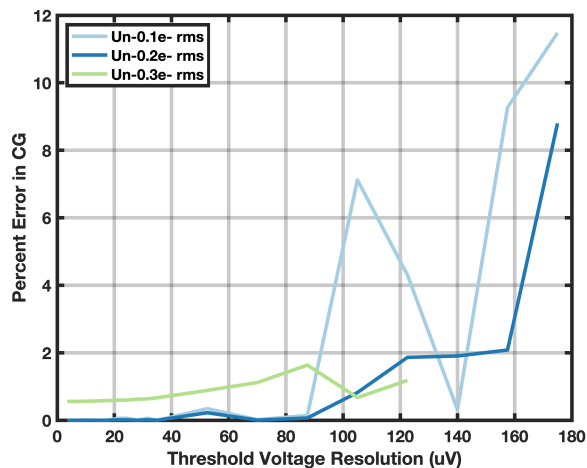

Figure 3: Simulated error in extracted CG as a function of threshold voltage sweep step size for different read noise.
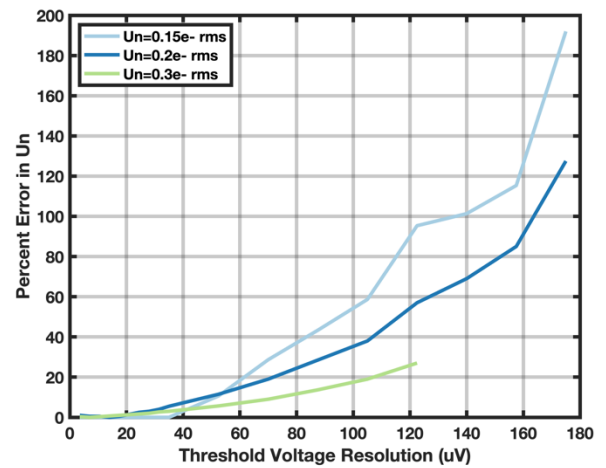

Figure 4: Simulated error in extracted read noise as a function of threshold voltage sweep step size for different read noise.
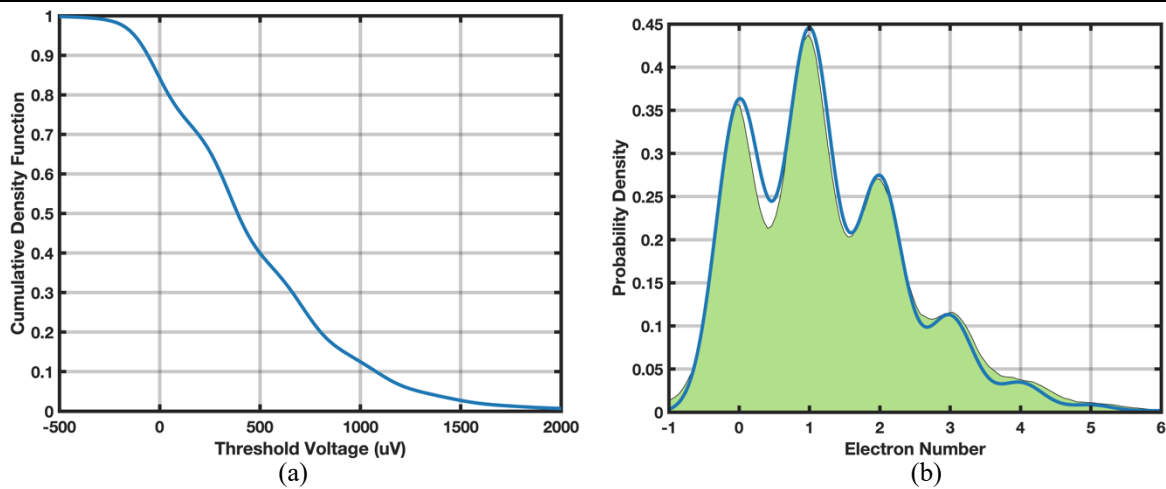
Figure 5: (a) CDF calculated using the data from a full 1024x1024 frame of analog pixel data. (b) Recovered photon counting histogram using numerical differentiation with its resulting curve fit.
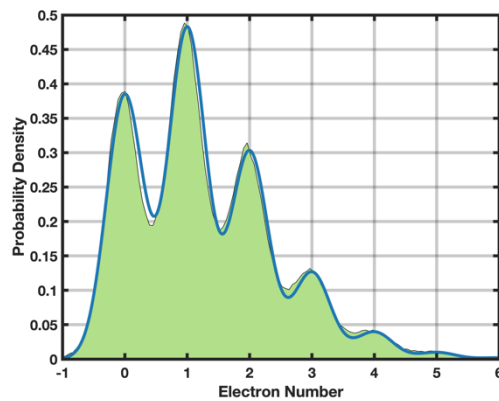

Figure 6: Recovered photon counting histogram using the same CDF as in Figure 5(a) using per pixel CG calibration to show improved matching with theoretical curve.

Figure 7: Comparison of images taken using the QIS camera module using either global CG calibration (normal) or per pixel CG calibration (calibrated) for different image pixel sizes.